New approach to a constant beamwidth transducer

Peter H. Rogers and A. L. Van Buren

Naval Research Laboratory, Underwater Sound Reference Division, Orlando, Florida 32856
(Received 29 June 1977; revised 14 December 1977)

The theory of a broadband constant beamwidth transducer which is to be used primarily as a projector is presented. The transducer is a spherical cap of arbitrary half angle α shaded so that the normal velocity is equal to $U_0 P_\nu(\cos\theta)$, where P_ν is the Legendre function whose root of smallest angle occurs at $\theta = \alpha$. The required value for ν, the order of the Legendre function (which is not, in general, an integer) can be obtained to within 1% for $\alpha \leq 1$ radian from the approximation $\nu \simeq 0.5[(4.81/\alpha) - 1]$. The transducer is shown to have uniform acoustic loading, extremely low sidelobes, and an essentially constant beam pattern for all frequencies above a certain cutoff frequency. Under piezoelectric drive the transducer is shown to have a flat transmitting current response over a broad band.

PACS numbers: 43.88.Ar, 43.20.Rz, 43.30.Jx, 43.30.Yj

INTRODUCTION

Most directional acoustic transducers and arrays exhibit beam patterns which are frequency dependent. (For example, the beamwidth of a plane piston or line array decreases with increasing frequency.) As a result, the spectral content of the transmitted (or received) signal will vary with position in the beam, and thus the fidelity of an underwater acoustic system will depend on the relative orientation of the transmitter and receiver. It would, therefore, be desirable to have a broadband directional transducer whose beam pattern is essentially independent of frequency over its bandwidth. With such a "constant beamwidth transducer" (CBT) the spectral content of the acoustic signal would be independent of bearing. A number of authors[1–6] have proposed (and built) more or less successful CBTs, but these involved the use of arrays of elements which were either interconnected by elaborate filters,[1–3] compensating networks,[3] or delay lines[4,5] or deployed in a complicated three-dimensional pattern,[6] and are thus more suitable as receivers than projectors. Moreover, all of these papers concerned devices which exhibited "constant" beamwidths over a limited bandwidth. The present paper presents a simple method for obtaining a CBT that is primarily to be used as a projector and accordingly will have a flat transmitting current response over a broad (but limited) bandwidth. The constant beamwidth characteristics of this transducer, however, extend over a bandwidth which is, in theory, virtually unlimited.

There are many possible applications for such a projector.

(1) *Broadband echo ranging.* Considerably more information about a target can be ascertained if broadband signals are employed. From the shape of the returned pulse one can infer the size, shape, and construction of the target. A relatively narrow beam is desirable in order to obtain the target bearing, avoid reverberation, and exclude extraneous targets. A CBT is required since the target will not always be located directly in the center of the beam.

(2) *High-data-rate communication.* High-data-rate underwater communication requires a broad bandwidth carrier. If for reasons of security or power limitation a directional sound beam is used, a constant beamwidth transducer is necessary to avoid loss of information due to misalignment of the transmitter and receiver. Good alignment may be difficult to achieve if the information is to be exchanged between two platforms, one or both of which may be in motion.

(3) *Broadband ultrasonic transducers for nondestructive testing, medical diagnosis, and materials research.* The fidelity of the transmitted and received signals affects the accuracy of derived parameters from flaws, tissue, and materials. The constant beam characteristics hold for the nearfield as well as for the farfield, thus making the application to highly directive ultrasonic transducers possible.

I. THEORY

It is well known[7–9] that if the radial velocity on the surface of a rigid sphere of radius a is equal to $U_0 u(\theta) \times e^{-i\omega t}$, where ω is the angular frequency, then the corresponding acoustic pressure will be

$$p(R,\theta,t) = i\rho c U_0 e^{-i\omega t} \sum_{n=0}^{\infty} A_n P_n(\cos\theta) \frac{h_n(kR)}{h_n'(ka)} , \qquad (1)$$

where R and θ are spherical coordinates, h_n is a spherical Hankel function, h_n' is its derivative, ρ is the density and c the sound speed of the surrounding fluid, and $k = \omega/c$ is the wave number. The quantity U_0 is the peak velocity, and $u(\theta)$ is the dimensionless velocity distribution. The quantities A_n are the coefficients in the expansion of $u(\theta)$ in the following series of Legendre polynomials $P_n(\cos\theta)$,

$$u(\theta) = \sum_{n=0}^{\infty} A_n P_n(\cos\theta) , \qquad (2)$$

and are defined by

$$A_n = (n + \tfrac{1}{2}) \int_0^{\pi} u(\theta) P_n(\cos\theta) \sin\theta \, d\theta . \qquad (3)$$

The farfield pressure, defined as the limit of $p(R,\theta,t)$ when $R \to \infty$, is written as

$$p_{FF}(R,\theta,t) = (\rho c U_0 a e^{ik(R-a)}/R) e^{-i\omega t} g(\theta) , \qquad (4)$$

where the angular dependence (beam pattern) $g(\theta)$ is given by

$$g(\theta)=\frac{e^{ika}}{ka}\sum_{n=0}^{\infty}\frac{A_n P_n(\cos\theta)}{i^n h_n'(ka)} \quad . \tag{5}$$

If the velocity distribution is a single complete Legendre polynomial, i.e., if $u(\theta)=P_l(\cos\theta)$, $l=0, 1, 2, \ldots$, for all θ, then the beam pattern is equal to $P_l(\cos\theta)$ at all frequencies. This beam pattern is, in fact, just the multipole beam pattern for a 2^l-pole which is, of course, frequency independent. However, a multipole pattern may not be desirable, because of very large sidelobes.

If the velocity distribution is other than a Legendre polynomial, the beam pattern is frequency dependent. Morse and Ingard[7] consider this case and conclude that the beam pattern approaches $u(\theta)$ in the limit as ka approaches infinity. Their analysis begins with the assumption that all coefficients A_n, $n>N$, are negligible in the series for $u(\theta)$ given in Eq. (2). Then only terms for $n\leq N$ need be included in the series for the beam pattern given in Eq. (5). When the frequency is high enough so that the Hankel functions $h_n'(ka)$, $n\leq N$, are approximately equal to their asymptotic form, they obtain

$$\begin{aligned} &g(\theta)\simeq\sum_{n=0}^{\infty}A_n P_n(\cos\theta)\ , \\ &g(\theta)\simeq u(\theta)\ , \end{aligned} \tag{6}$$

so that the beam pattern is approximately equal to the surface velocity distribution. The rate at which $g(\theta)$ approaches $u(\theta)$ with increasing frequency depends on $u(\theta)$. We define $\mathcal{L}$ to be the lowest value of ka for which Eq. (6) applies and call it the cutoff frequency for the associated velocity distribution. The lower the order of the last Hankel function $h_N'(ka)$ required in Eq. (5), the smaller the value of ka for which all the included Hankel functions $h_n'(ka)$, $n\leq N$, are approximately equal to their asymptotic forms. Thus the more rapidly the Legendre coefficients A_n decrease to a negligible value, the lower the cutoff frequency for the corresponding velocity distribution. Each velocity distribution has its own unique set of expansion coefficients and its own cutoff frequency.

We are interested in velocity distributions $u(\theta)$ that are equal to zero for all angles greater than a given value θ_0. The corresponding farfield radiation will be restricted to the angular cone $\theta\leq\theta_0$ for $ka\geq\mathcal{L}$. Let $f(\theta)$ be the analytic function which equals $u(\theta)$ for $0\leq\theta<\theta_0$. We wish to determine the function $f(\theta)$ which minimizes $\mathcal{L}$ for a given value of θ_0. Therefore, we seek the function $f(\theta)$ whose Legendre coefficients $|A_n|$ decrease most rapidly. For this case A_n is given by Eq. (3) with $u(\theta)$ replaced by $f(\theta)$ and the upper limit replaced by θ_0. We can obtain a relationship between θ_0 and $f(\theta)$ by examining the extrema of each A_n^2 with respect to θ_0. Setting the first derivative $\partial A_n^2/\partial\theta_0$ equal to zero yields the requirement that

$$f(\theta_0)P_n(\cos\theta_0)A_n=0\ . \tag{7}$$

Since $P_n(\cos\theta_0)$ and A_n are normally not zero, satisfaction of Eq. (7) for all n requires that $f(\theta_0)=0$. Therefore, we must truncate the velocity distribution at one of the roots of $f(\theta)$. We choose the smallest root in order to avoid introducing sidelobes in the beam pattern.

Additional information about $f(\theta)$ can be obtained by examining the second derivative $\partial^2A_n^2/\partial\theta_0^2$, to determine whether the extrema for A_n^2 associated with $f(\theta_0)=0$ are minima or maxima. The second derivative is given by

$$\frac{\partial^2A_n^2}{\partial\theta_0^2}=(2n+1)f'(\theta_0)P_n(\cos\theta_0)A_n\sin\theta_0\ . \tag{8}$$

The smallest root of $P_n(\cos\theta)$ decreases monotonically with increasing n. We can, therefore, define an n' such that for all $n<n'$ the smallest root of $P_n(\cos\theta)$ will be greater than θ_0. Thus, for $n<n'$, $P_n(\cos\theta)$ is positive for $\theta\leq\theta_0$ and from Eq. (3) A_n must also be positive. Since both $P_n(\cos\theta_0)$ and A_n are positive and $f'(\theta)$ is negative in our case, the second derivative must be negativ for $n<n'$. For $n>n'$ the second derivative may be either positive or negative. The second derivative will be positive when the following inequality holds:

$$P_n(\cos\theta_0)\int_0^{\theta_0}f(\theta)P_n(\cos\theta)\sin\theta\,d\theta<0\ ,\quad n>n'\ . \tag{9}$$

A solution to inequality (9) is $f(\theta)=P_\nu(\cos\theta)$, where the Legendre function order ν is the smallest positive number for which $P_\nu(\cos\theta_0)=0$. We note that ν will not, in general, be an integer. The lower bound n' is the integer truncation of ν. For this choice of $f(\theta)$ the coefficients A_n are given by

$$\begin{aligned} A_n=&-[(1-\cos^2\theta_0)/(n-\nu)(n+\nu+1)] \\ &\times P_n(\cos\theta_0)P_\nu'(\cos\theta_0)\ ,\quad n\neq\nu\ , \end{aligned} \tag{10}$$

and the second derivative is given by

$$\begin{aligned} \frac{\partial^2A_n^2}{\partial\theta_0^2}=&(2n+1)\frac{(1-\cos^2\theta_0)}{(n-\nu)(n+\nu+1)} \\ &\times[P_n(\cos\theta_0)P_\nu'(\cos\theta_0)]^2\ ,\quad n\neq\nu\ , \end{aligned} \tag{11}$$

where the prime on $P_\nu'(\cos\theta_0)$ denotes differentiation with respect to $\cos\theta_0$. For the special case where ν is an integer, the expression for the coefficient A_n, $n=\nu$, can be obtained from the limit of the right hand side of Eq. (10) as ν approaches n.

We see from Eq. (11) that the second derivative is always negative for $n<\nu$ and always positive for $n>\nu$. Therefore, the Legendre function $P_\nu(\cos\theta)$ truncated at its first zero θ_0 maximizes A_n^2 as a function of θ_0 for $n<\nu$ while simultaneously minimizing A_n^2 as a function of θ_0 for $n>\nu$. The effect is to concentrate the energy of $u(\theta)$ in the lower-order terms of its Legendre series expansion, thereby allowing for rapid decrease in the magnitude of the higher-order terms and minimization of the cutoff frequency.

Thus, if we have the surface velocity distribution

$$\begin{aligned} &u(\theta)=P_\nu(\cos\theta)\ ,\quad \theta\leq\theta_0 \\ &u(\theta)=0\ ,\quad \theta\geq\theta_0\ , \end{aligned} \tag{12}$$

we will obtain to a good approximation the farfield beam pattern

$$\begin{aligned} &g(\theta)\simeq P_\nu(\cos\theta)\ ,\quad \theta\leq\theta_0 \\ &g(\theta)\simeq 0\ ,\quad \theta\geq\theta_0\ , \end{aligned} \tag{13}$$

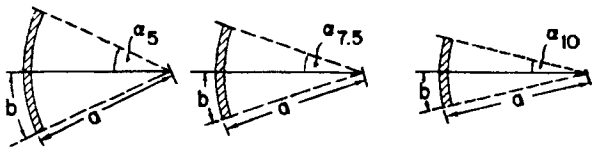

FIG. 1. Geometry of P_5 CBT (left), $P_{7.5}$ CBT (center), and P_{10} CBT (right).

for $ka \geq \mathcal{L}$, where the minimized cutoff frequency $\mathcal{L}$ depends on the order ν. The Legendre function $P_\nu(\cos\theta)$, $\nu > 0$, is equal to one at $\theta = 0$ and has its first root at the angle $\theta_0 = \alpha_\nu$. The value for α_ν decreases monotonically with increasing ν, i.e., the higher the value of ν the narrower the beam. A good approximation for $P_\nu(\cos\theta)$, $0 \leq \theta \leq \alpha_\nu$, is given by the first term of the Bessel function series expansion of P_ν derived by Szegö[10]:

$$P_\nu(\cos\theta) \simeq (\theta/\sin\theta)^{1/2} J_0[(\nu + 0.5)\theta] . \tag{14}$$

Using the known first root of J_0 together with a correction term necessary for small values of ν, we obtain the approximation

$$\alpha_\nu \simeq \frac{2.405}{\nu + 0.5}\left[1 - \frac{0.045}{(\nu + 0.5)^2}\right] . \tag{15}$$

This approximation improves with increasing ν, being correct to within 0.1% for $\nu \geq 1$. Inverting Eq. (15) we obtain an approximation for the order ν in terms of α_ν:

$$\nu \simeq 0.5\,[(4.81/\alpha_\nu)(1 - 0.0081\,\alpha_\nu^2) - 1] . \tag{16}$$

This approximation improves with decreasing α_ν and is correct to within 0.1% for $\alpha_\nu \leq \pi/2$. The simpler approximation $\nu \simeq 0.5\,[(4.81/\alpha_\nu) - 1]$ is accurate to within 1% for $\alpha_\nu \leq 1$ radian.

We define $\mathcal{L}$ as the lowest value of ka for which the derivative of the largest order Hankel function $h_N'(ka)$ retained in the series Eq. (5) is approximately equal to its asymptotic form. Examination shows that this requires that $[1 + 0.5N(N+1)]/ka$ be small compared to unity. The pressure on the surface of the sphere is given by Eq. (1) with R set equal to a. The angular dependence of the surface pressure $g_a(\theta)$ will be approximately equal to the velocity distribution $u(\theta)$ if $h_N(ka)/h_N'(ka)$ is approximately equal to its asymptotic form. This requires that $\{1 - [1 - 0.5N(N+1)]/ka\}/ka$ be small compared to unity, a condition less restrictive than for the farfield pressure. Examination of the corresponding ratio $h_N(kR)/h_N'(ka)$ for intermediate distances R shows that the condition required for this ratio to be approximately equal to its asymptotic form becomes progressively less restrictive as R approaches a. Thus we find that both the surface and nearfield pressure distributions approach the surface velocity distribution more rapidly with increasing ka than does the farfield beam pattern. Consequently for $ka \geq \mathcal{L}$ the angular dependence of the pressure $g_R(\theta)$ at any distance $R \geq a$ is given to a good approximation by

$$\begin{aligned} g_R(\theta) &\simeq P_\nu(\cos\theta) , \quad \theta \leq \alpha_\nu \\ g_R(\theta) &\simeq 0 , \quad \theta \geq \alpha_\nu . \end{aligned} \tag{17}$$

One significant consequence of this result is that the specific acoustic radiation impedance everywhere on the active part of the sphere is essentially equal to ρc. A second significant consequence is obtained in the case where the sphere is a rigid spherical shell whose inside normal surface velocity is equal to zero. Then, since both the surface pressure and velocity are nearly zero over the inactive part of the outside surface of the sphere, the part of the spherical shell for $\theta \geq \alpha_\nu$ can be removed without significantly changing the acoustic fields, i.e., the constant beamwidth behavior would still exist. Thus we need retain only the active spherical cap of cone angle α_ν. The radius of this cap (the primary dimension of the transducer) is given by

$$b = a\,\alpha_\nu . \tag{18}$$

It is appropriate to redefine the cutoff frequency in terms of kb instead of ka. Thus we replace the condition $ka \geq \mathcal{L}$ with the equivalent condition $kb \geq \Omega_\nu$ and in the remainder of the paper refer to Ω_ν as the cutoff frequency. The relative sizes of a, b, and the curvature of the transducer for $\nu = 5$, 7.5, and 10 are shown in Fig. 1. The appropriate velocity distributions for these three cases as given by Eq. (12) are shown in Fig. 2.

It is difficult to obtain analytically an exact expression for the cutoff frequency Ω_ν. One approach to determining Ω_ν stems from the intuitive requirement that the spherical cap must be large enough to support a sound beam of the required width. The first null for the P_ν beam pattern occurs at α_ν. The first null for a plane piston of radius a_p occurs at[11]

$$\theta = \sin^{-1}(3.831/ka_p) \simeq 3.83/ka_p . \tag{19}$$

The equivalent plane piston required to produce a null at α_ν would thus have a radius given by

$$a_p = 3.83/k\alpha_\nu \simeq [(2\nu + 1)/k](3.83/4.81) ; \tag{20}$$

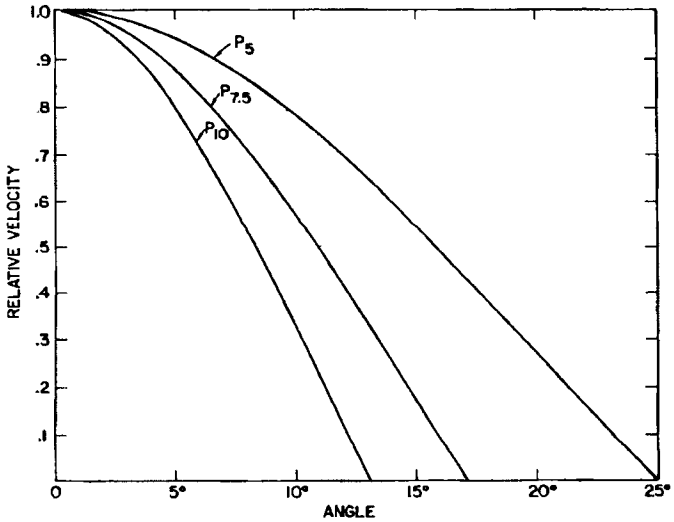

FIG. 2. Velocity shading functions [from Eq. (12)] for $\nu = 5$, 7.5, and 10.

hence we require

$$kb \geq (8\nu+4)/5 \ . \tag{21}$$

This condition, however, turns out to be a little weak for small ν because the shading reduces the effective size of the piston and because the curvature is relatively large for small ν. A general rule of thumb, however, can be obtained by adding an empirically determined constant to Eq. (21):

$$kb \geq \Omega_\nu \equiv (8\nu+27)/5. \tag{22}$$

We enumerate the expected properties of the P_ν CBT for $kb \geq \Omega_\nu$:

(1) Essentially constant beam pattern.

(2) Very low sidelobes.

(3) The surface pressure distribution as well as the pressure distribution at all distances out to the far-field is approximately equal to the surface velocity distribution. Thus, in a sense, there is no nearfield.

(4) Since both the surface velocity and surface pressure have the same dependence on θ, the local specific acoustic radiation impedance is independent of θ (and equal to ρc). Thus the entire transducer is uniformly loaded. This is particularly important if the transducer is to be made in the form of a mosaic of small transducers operated near resonance.

(5) Many directional piezoelectric transducers are essentially constant velocity devices over a wide frequency range below resonance. Over this range they exhibit a 6 dB/octave rise in transmitting current response directly attributable to the increasing directivity index (DI). This results in a flat voltage receiving sensitivity when used as a hydrophone. A CBT of similar construction, which would have a constant DI in addition to a constant radiation impedance, would thus have a broad band below resonance over which its *transmitting* current response would be flat.

II. NUMERICAL TEST

We tested our hypothesis by numerically calculating the acoustic pressure produced by a spherical radiator. We used the series expansions given in Eqs. (1) and (5). Depending on the particular case, up to 200 terms were retained in the series. (We note that we are actually analyzing a shaded spherical cap in a rigid spherical baffle. However, arguments given earlier in Sec. I show that the presence or absence of the baffle should not significantly affect the acoustic fields for $kb \geq \Omega_\nu$.) The coefficients A_n were normally evaluated by use of Eq. (10). For the special case where ν is an integer the single coefficient A_n, $n=\nu$, was evaluated by expressing $P_\nu^2(x)$ as a polynomial in x and integrating term by term. A good approximation for this coefficient can be obtained by using for $P_\nu(\cos\theta)$ the approximation given in Eq. (14), integrating exactly the resulting expression, and adding an empirically determined correction necessary for low ν:

$$A_\nu \simeq [1.5586/(2\nu+1)][1-0.345/(2\nu+1)^2] \ . \tag{23}$$

This approximation improves with increasing ν, being accurate to within 0.1% for $\nu \geq 1$. It can be shown that the DI for a P_ν CBT is given in terms of A_ν as follows:

$$\mathrm{DI} = -10\log[A_\nu/(2\nu+1)] \ . \tag{24}$$

Here A_ν is defined by Eq. (23) with ν allowed to be non-integer.

All of the Legendre polynomials and Hankel functions required in the numerical calculations were obtained by use of standard recursion relations. We replace $P_\nu'(\cos\alpha_\nu)$ required for the calculation of A_n with the equivalent expression $[\nu P_{\nu-1}(\cos\alpha_\nu)/(1-\cos^2\alpha_\nu)]$ and evaluated $P_{\nu-1}(\cos\alpha_\nu)$ using its hypergeometric series in $\frac{1}{2}(1-\cos\alpha_\nu)$.

The computer analyses have been carried out for the cases of P_5, $P_{7.5}$, and P_{10}. The geometries are shown in Fig. 1. The input shading functions are shown in Fig. 2. For a P_5 CBT the spherical cap has the cone angle $\alpha_5 = 25.02°$; for a $P_{7.5}$ CBT, $\alpha_{7.5} = 17.22°$; and for a P_{10} CBT, $\alpha_{10} = 13.12°$. From Fig. 2 we see that the shading function is almost linear with angle toward the edge of the cap.

The results for the P_5 CBT are summarized in Figs. 3 through 5. In the bottom half of Fig. 3 we see the -6- and -3-dB half beamwidths for the P_5 CBT plotted as a function of kb. For $kb \geq \Omega_5$ the total variation in the -3- or -6-dB beamwidth is less than about $\pm 2°$ and less than about $\pm 1°$ for $kb \geq 2\Omega_5$. The piezoelectric (constant velocity) transmitting current response for a P_5 CBT is shown on the top half of Fig. 3 and on Fig. 4. Above $kb = \Omega_5$ it is flat to within about ± 1 dB. Well below $kb = \Omega_5$ the response rises 6 dB/octave. The corresponding curve for a plane circular piston would continue to rise 6 dB/octave for all values of kb, while the corresponding curve for a 25° unshaded spherical cap would have maxima 6 dB above the 0-dB level and near nulls for minima. (See Fig. 4.)

We note that the constant velocity transmitting current response for the unshaded spherical cap does not

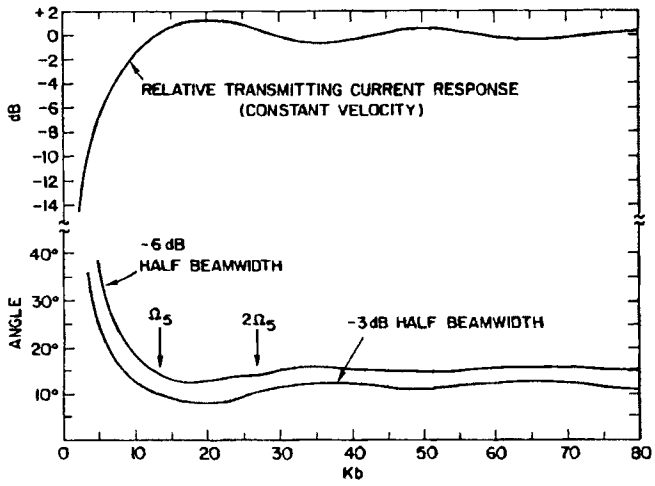

FIG. 3. Relative constant velocity transmitting current response (top) and -3- and -6-dB half beamwidth (bottom) for P_5 CBT as a function of kb.

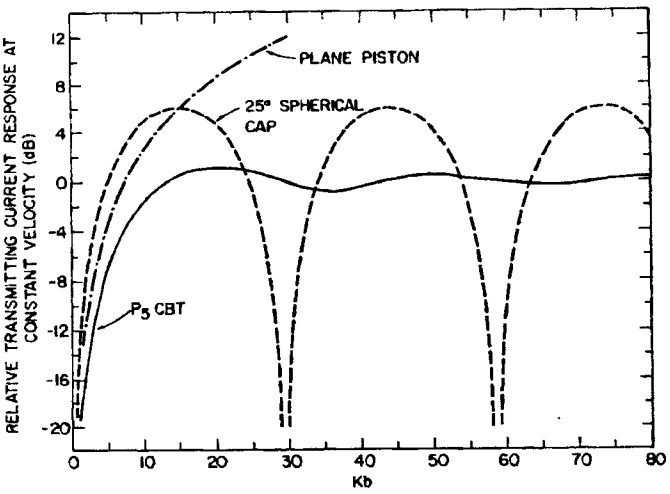

FIG. 4. Comparison of constant velocity transmitting current response of P_5 CBT with circular plane piston and 25° spherical cap.

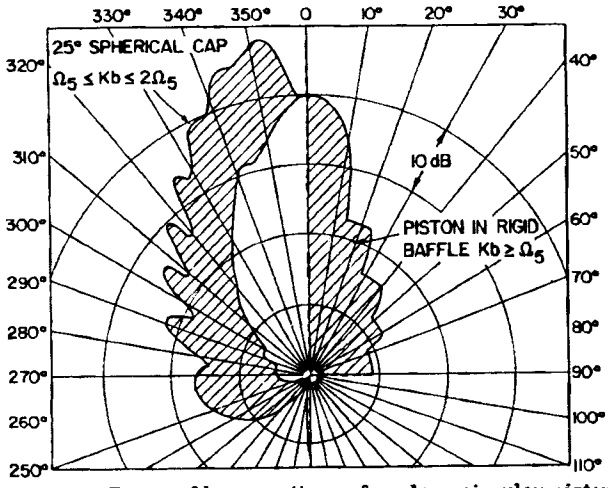

FIG. 6. Range of beam patterns for plane circular piston for $kb \ge \Omega_5$ (right) and 25° spherical cap for $\Omega_5 \le kb \le 2\Omega_5$.

approach a constant value in the limit of large frequency. The alternate maxima and minima shown in Fig. 4 repeat indefinitely as kb approaches infinity. The position of the extrema can be determined very accurately by requiring that the height of the cap $a(1-\cos 25°)$ be equal to an integral number of half wavelengths $m\lambda/2$. Odd values of m correspond to minima, and even values correspond to maxima.

The corresponding beam patterns show an interference peak or valley centered around 0°. As the frequency increases to large values, the pressure around 0° alternately rises and falls relative to the rest of the pattern. The angular width of the peak or valley decreases with increasing frequency. The pressure outside the paraxial region behaves normally; it approaches a stable value and its distribution approaches the velocity distribution. Thus it appears that the uniformly shaded cap is an exception to the rule that the beam pattern always approaches the velocity distribution as the frequency increases indefinitely. The width of the exceptional region does decrease toward zero but the region always includes the important $\theta = 0°$ value. The initial assumption of Morse and Ingard[7] leading to Eq. (6) does not apply to the uniformly shaded cap since the corresponding Legendre coefficients $|A_n|$ decrease so slowly with increasing n that for $\theta \simeq 0°$ the series of Eq. (5) does not converge until n becomes larger than ka and $h_n'(ka)$ increases rapidly to force convergence. The extent of the deviation from a constant beam pattern is illustrated in Fig. 5. For all frequencies such that $kb \ge \Omega_5 = 13.4$ *all* beam patterns will fall within the hatched area shown in Fig. 5. For $kb \ge 2\Omega_5$ all beam patterns fall within the much more restricted region indicated by the crosshatched area in Fig. 5. We note that within the 40-dB dynamic range used in Fig. 5 no secondary lobes appear in either the extrema shown here or in any of the single-frequency beam patterns used to obtain the extrema. Use of a larger dynamic range would show that the only noticeable secondary lobe is a backlobe due to the "hot spot" at $\theta = 180°$. The level of this backlobe decreases with increasing frequency, having a value of -48 dB at $kb = \Omega_5$ and -60 dB at $kb = 2\Omega_5$. For comparison the right hand side of Fig. 6 shows the extent of variation of the beam patterns for a plane circular piston for $kb \ge \Omega_5$ while the left hand side shows the extent of variation of the beam patterns for a 25° spherical cap in the *bounded* region $\Omega_5 \le kb \le 2\Omega_5$.

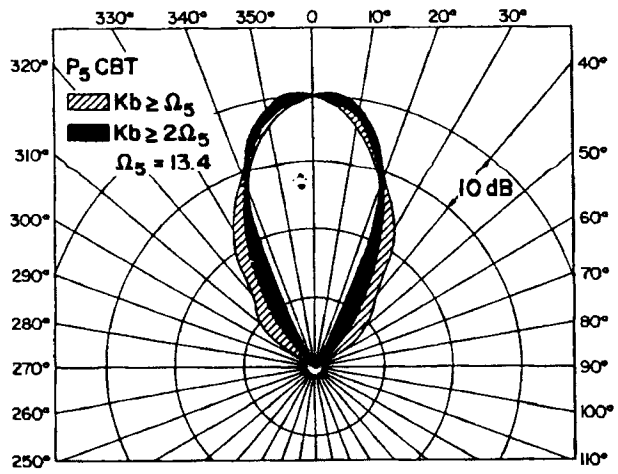

FIG. 5. Range of beam patterns for P_5 CBT for $kb \ge \Omega_5$ (hatched area) and $kb \ge 2\Omega_5$ (cross-hatched area).

Figure 7 shows the extent of deviation from constant beam pattern for the $P_{7.5}$ CBT for $kb \ge \Omega_{7.5} = 17.4$ (hatched area) and $kb \ge 2\Omega_{7.5}$ (cross-hatched area). Note that the beam patterns are all narrower than they were for the P_5 CBT though, of course, it must be remembered that $\Omega_{7.5} > \Omega_5$. The most pronounced secondary lobe, although unnoticeable in Fig. 7, is the backlobe with a level of -60 dB at $kb = \Omega_{7.5}$ and -69 dB at $kb = 2\Omega_{7.5}$. Similarly, Fig. 8 shows the extent of deviation from constant beamwidth for a P_{10} CBT. All beam patterns for $kb \ge \Omega_{10} = 21.4$ fall within the hatched area in Fig. 8 and all beam patterns for $kb \ge 2\Omega_{10}$ fall within the cross-hatched area. Again the sidelobes are virtually nonexistent. The backlobe is down 70 dB at $kb = \Omega_{10}$ and 88 dB at $kb = 2\Omega_{10}$. Figures 3, 5, 7, and 8 indicate that if Legendre shading can indeed be achieved on a

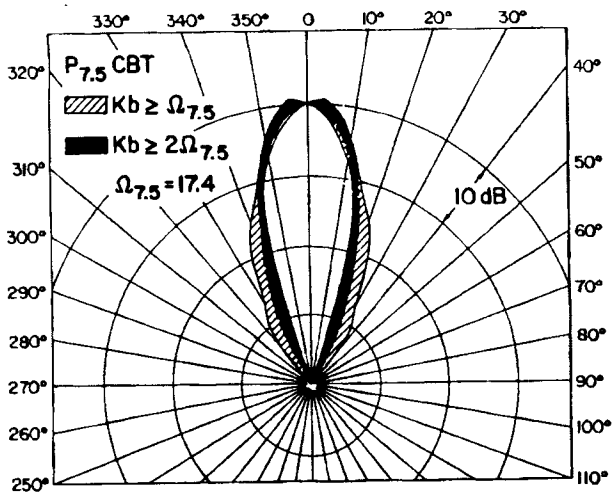

FIG. 7. Range of beam patterns for $P_{7.5}$ CBT for $kb \geq \Omega_{7.5}$ (hatched area) and $kb \geq 2\Omega_{7.5}$ (cross-hatched area).

spherical cap the transducer will exhibit CBT characteristics. Small errors (up to ± 5%) have been introduced into the shading without appreciably disturbing these CBT characteristics. It is, however, essential for the normal velocity to be very nearly zero at α_ν to avoid large deviations from constant beamwidth due to the superposition of the erratic patterns of an unshaded spherical cap and the CBT patterns. We calculated the pressure on the surface of the sphere for all three cases considered above and confirmed that the surface pressure distribution more closely matches the velocity distribution than does the beam pattern. As an example we show in Fig. 9 the comparison of the surface pressure distribution, beam pattern, and velocity distribution for a P_5 CBT at $kb = \Omega_5$. The surface pressure distribution is normalized by $\rho c U_0$.

The constant beamwidth results described above for a rigid spherical cap can be shown to apply equally well to an acoustically transparent spherical shell. However, the acoustic radiation from a transparent spherical cap is bidirectional. A constant beamwidth pressure distribution matching the velocity distribution on the cap is produced in both the forward ($\theta = 0°$) and the backward ($\theta = 180°$) directions. Trott[12] applied the results presented in an earlier unpublished version of the present paper to the theoretical design of a receiver CBT using $P_1(\cos\theta) = \cos\theta$ shading on an acoustically transparent hemispherical cap.

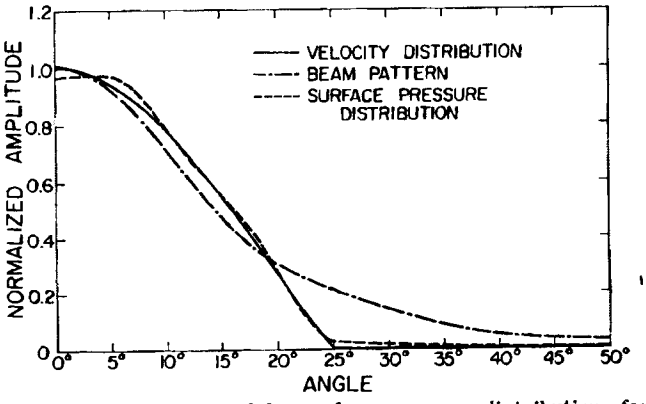

FIG. 9. Comparison of the surface pressure distribution, far-field beam pattern, and velocity distribution for P_5 CBT for $kb = \Omega_5$.

III. CONCLUSIONS

We have shown, in theory, that a satisfactory CBT projector can be constructed from a piezoelectric spherical cap of arbitrary half angle α_ν whose normal velocity is shaded in the form of the Legendre function $P_\nu(\cos\theta)$ whose root of smallest angle occurs at $\theta = \alpha_\nu$. For $kb \geq \Omega_\nu$ the transducer will exhibit uniform loading, extremely low sidelobes, and a beam pattern which is essentially independent of both frequency and distance from the source.

ACKNOWLEDGMENT

The authors are indebted to W. J. Trott who first suggested amplitude shading of a spherical transducer as the basis for a CBT.

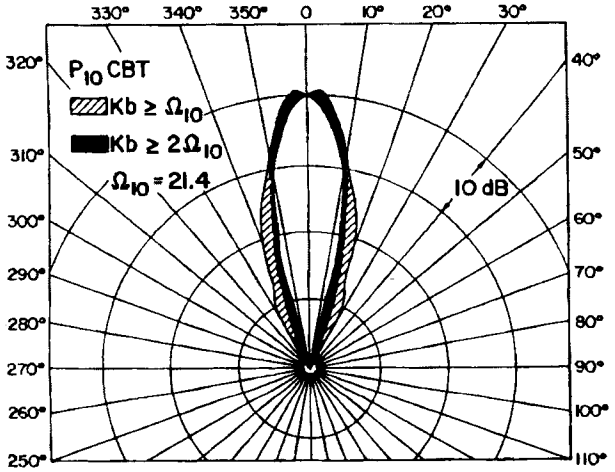

FIG. 8. Range of beam patterns for P_{10} CBT for $kb \geq \Omega_{10}$ (hatched area) and $kb \geq 2\Omega_{10}$ (cross-hatched area).

[1]E. L. Hixson and K. T. Au, J. Acoust. Soc. Am. 48, S117(A) (1970).
[2]R. J. Holden and E. L. Hixson, J. Acoust. Soc. Am. 51, S106(A) (1972).
[3]R. P. Smith, Acustica 23, 21–26 (1970).
[4]D. G. Tucker, Nature (London) 180, 496 (1957).
[5]J. C. Morris and E. Hands, Acustica 11, 341–347 (1961).
[6]J. C. Morris, J. Sound Vib. 1, 28–40 (1964).
[7]P. M. Morse and K. U. Ingard, *Theoretical Acoustics* (McGraw–Hill, New York, 1968), pp. 338–341.
[8]H. Stenzel, *Leitfaden Zur Berechnung von Schallvorgangen* (Springer–Verlag, Berlin, 1939).
[9]C. T. Molloy, J. Acoust. Soc. Am. 43, 592–609 (1968).
[10]See, for example, A. Erdelyi, W. Magnus, F. Oberhettinger, and F. Tricomi, *Higher Transcendental Functions* (McGraw–Hill, New York, 1953), Vol. 2 of the Bateman Manuscript Project, p. 58.
[11]W. B. Stephens and A. E. Bates, *Acoustics and Vibrational Physics* (St. Martins, New York, 1966), p. 714.
[12]W. J. Trott, "Design Theory for a Constant-Beamwidth Transducer," Nav. Res. Lab. Rep. No. 7933 (1975).